British Journal of Pharmacology (2007) 151, 952–962
 0007–1188/07 $30.00
www.brjpharmacol.org

RESEARCH PAPER

Molecular characterisation of the interactions between olmesartan and telmisartan and the human angiotensin II AT_1 receptor

MT Le[1], MK Pugsley[2], G Vauquelin[1] and I Van Liefde[1]

[1]*Departments of Molecular and Biochemical Pharmacology, Free University of Brussels (VUB), Brussels, Belgium and* [2]*Department of Pharmacology, Forest Research Institute, Jersey City, NJ, USA*

Background and purpose: Whereas some angiotensin II (Ang II) type 1 receptor blockers (ARBs) produce surmountable antagonism of AT_1 receptors, others such as olmesartan and telmisartan display varying degrees of insurmountability. This study compared the molecular interactions of olmesartan and telmisartan with the human AT_1 receptor, using well characterised *in vitro* methods and model systems.
Experimental approach: CHO-K1 cells that stably express human AT_1 receptors (CHO-hAT_1 cells) were used in several pharmacological studies of olmesartan and telmisartan, including direct radioligand binding and inhibition of Ang II-induced inositol phosphate (IP) accumulation.
Key results: Both ARBs were found to be competitive antagonists that displayed high affinity, slow dissociation, and a high degree of insurmountability for the AT_1 receptor (the latter greater with olmesartan). Their receptor interactions could be described by a two-step process with the initial formation of a loose complex (IR) and subsequent transformation into a tight binding complex (IR*). In washout experiments, [^{3}H] telmisartan dissociated from the receptor with a half-life of 29 min and the Ang II-mediated IP accumulation response was 50% maximally restored within 24 min, whereas values for [^{3}H] olmesartan were 72 min and 76 min, respectively.
Conclusions and implications: The high degree of insurmountability, slow dissociation, and high affinity of olmesartan for its receptor may relate to its ability to stabilise IR* via the carboxyl group of its imidazole core. In comparison, telmisartan displays a less potent interaction with the receptor.
British Journal of Pharmacology (2007) **151,** 952–962; doi:10.1038/sj.bjp.0707323; published online 18 June 2007

Keywords: angiotensin II; AT_1 receptor; olmesartan; telmisartan; losartan; EXP3174; receptor interactions; insurmountability

Abbreviations: Ang II, angiotensin II; ARB, angiotensin II receptor blocker; CHO, Chinese hamster ovary; DMEM, Dulbecco's modified essential medium; hAT_1 or AT_1, human angiotensin II type 1 receptor; IP, inositol phosphate; RAAS, renin–angiotensin–aldosterone system

Introduction

The renin–angiotensin–aldosterone system (RAAS) plays a key role in blood pressure modulation and in the pathogenesis of hypertension. Angiotensin II (Ang II), the primary product of the RAAS enzyme cascade, binds to the type 1 (AT_1) receptor (de Gasparo *et al*., 2000) mediating vasoconstriction of vascular smooth muscle, aldosterone secretion from adrenal glomerulosa cells (promoting sodium and water retention), cellular proliferation and hypertrophy.

Orally-active, non-peptide-based Ang II receptor blockers (ARBs) that selectively antagonize the AT_1 receptor have been highly successful in the treatment of hypertension, renal disease and heart failure (Timmermans, 1999; Oparil, 2000; Manohar and Pina, 2003; Norris and Vaughn, 2003), and in reducing end-organ damage associated with diabetes and atherosclerosis (Gavras, 1999). Structurally, currently marketed ARBs consist of a substituted imidazole core containing a biphenylmethyl moiety with either an acidic tetrazole or carboxylic acid substituents at the 2′-position (Berellini *et al*., 2005; Mire *et al*., 2005). While all ARBs (including the active metabolite of losartan (EXP3174), although not losartan) bind with high affinity ($IC_{50} \approx 6.5$–16 nM) to the AT_1 receptor (Timmermans, 1999; Mire *et al*., 2005), distinct differences in the mode of interaction of ARBs with the receptor exist (Vauquelin *et al*., 2002, 2006). Marked differences in the competitive blockade of Ang II at the AT_1 receptor have been demonstrated (Cazaubon *et al*., 1993;

Correspondence: Professor G Vauquelin, Department of Molecular and Biochemical Pharmacology, Vrije Universiteit Brussel (VUB), Building E.5.10, Pleinlaan 2, B-1050 Brussels, Belgium.
E-mail: gvauquel@vub.ac.be
Received 22 January 2007; revised 15 March 2007; accepted 11 April 2007; published online 18 June 2007

Criscione *et al*., 1993; Noda *et al*., 1993; Wienen *et al*., 1993; Mizuno *et al*., 1995; Mochizuki *et al*., 1995) and while ARBs such as losartan, tasosartan and eprosartan produce surmountable antagonism of AT_1 receptors, others such as olmesartan, irbesartan, valsartan, E3174 and telmisartan display varying degrees of insurmountability (Timmermans, 1999; Vauquelin *et al*., 2002). The term insurmountable antagonism is used to indicate that an agonist's maximum effect is reduced by pretreatment with the antagonist. This type of antagonism can be attributed to several distinct molecular mechanisms, including irreversible or slow reversible competitive antagonism; noncompetitive antagonism; or functional antagonism (Neubig *et al*., 2003).

To explain the changes observed in dose–response curves for surmountable and insurmountable ARBs, a two-state, two-step antagonist AT_1 receptor kinetic model that relates to slow dissociation of the ARB from the AT_1 receptor has been proposed (Fierens *et al*., 1999b; Vanderheyden *et al*., 2000a; Vauquelin *et al*., 2001c, d). So, although all ARBs share a common mechanism of action, differences in molecular structure may contribute to differences in binding kinetics and pharmacological activity.

Olmesartan medoxomil is an ARB that has a rapid onset of action (Laeis *et al*., 2001), long-lasting antihypertensive efficiency observed in the clinic (Smith *et al*., 2005) and produces long-lasting inhibition of Ang II-mediated pressor responses. This may, in part, relate to its slow dissociation from the AT_1 receptor (Mire *et al*., 2005) as olmesartan produces selective, insurmountable inhibition of the AT_1 receptor (Yanagisawa *et al*., 1996; Koike *et al*., 2003). Structurally, olmesartan has a tetrazole group at the 2-position of the biphenyl moiety and, after de-esterification of the prodrug, a carboxyl group at the 5-position of the imidazole ring (a group thought to have a role in receptor insurmountability) (Noda *et al*., 1993; Mizuno *et al*., 1995). It also has a hydroxyalkyl substituent at the imidazole 4-position that is unique to olmesartan and contributes significantly to its high-affinity binding to the AT_1 receptor (Yanagisawa *et al*., 1996).

Telmisartan (BIBR 277) distinguishes itself among the other ARBs by its long plasma half-life (~24 h) (White *et al*., 2004) and has been reported to dissociate slowly from the AT_1 receptor (Maillard *et al*., 2002; Kakuta *et al*., 2005). Application of the two-state, two-step kinetic model for ARBs suggests that slow receptor dissociation should result in a high degree of insurmountability; (Vauquelin *et al*., 2001c) however, *in vitro* studies have shown that telmisartan produces only a ~50% reduction in the maximal Ang II-mediated response (Wienen *et al*., 1993; Schambye *et al*., 1994). Among the potential explanations for this discrepancy are structural differences compared with related ARBs. In particular, telmisartan has a carboxyl substitution instead of a tetrazole group in the biphenyl moiety and lacks heterocyclic substitution of the benzimidazole moiety, with no carboxyl group in the imidazole core (Ries *et al*., 1993; Berellini *et al*., 2005).

This study compares the molecular interactions of olmesartan and telmisartan with the human AT_1 receptor using well-characterized *in vitro* methods and model systems, and evaluates whether differences in their molecular structures could affect their binding properties.

Methods

Cell culture

Chinese hamster ovary (CHO) cells stably expressing the human Ang II type 1 receptor (CHO-hAT_1 cells) were cultured in 24-well plates in DMEM (Dulbecco's modified essential medium), which was supplemented with 10% fetal bovine serum, 2 mM L-glutamine, 100 IU ml^{-1} penicillin, 100 $\mu g\,ml^{-1}$ streptomycin, 1% (v v^{-1}) of a solution of non-essential amino acids and 1 mM sodium pyruvate (Life Technologies, Merelbeke, Belgium). CHO-hAT_1 cells were grown in 5% CO_2 at 37°C until confluence. The medium was replaced by DMEM supplemented with 1 $\mu Ci\,ml^{-1}$ myo[^{3}H] inositol and the cells were further grown for ~24 h in 5% CO_2 at 37°C.

Radioligand binding studies

Cells were initially washed three times with DMEM (~500 μl per well) at room temperature (22±2°C). Subsequently, 400 μl DMEM was added to each well for 15 min at 37°C. Incubations proceeded at 37°C and were initiated by adding 100 μl of DMEM containing either [^{3}H] olmesartan or [^{3}H] telmisartan. Each radiolabelled compound was added either alone or in presence of unlabelled antagonists at the indicated final concentrations. At the end of each of the incubations, the CHO-hAT_1 cells were briefly washed three times with Krebs-Ringer buffer (~500 μl per well) at 4°C. The cell-bound radioactivity in each well was determined by solubilization with 250 μl of 1 M sodium hydroxide and counted for 3 min in a liquid scintillation counter after the addition of 3 ml scintillation liquid (Optisafe, Wallac, Turku, Finland).

Kinetic experiments. For association binding, cells were incubated in 500 μl DMEM containing 1.5 nM [^{3}H] olmesartan for 5–90 min or with either 1.5 or 5.0 nM [^{3}H] telmisartan for 5–240 min at 37°C. Nonspecific binding was obtained in the presence of 0.2 μM unlabelled candesartan per 1 nM [^{3}H] olmesartan or [^{3}H] telmisartan. For dissociation experiments, cells were first incubated for 40 min with 1.5 nM [^{3}H] olmesartan or for 20 min with 5 nM [^{3}H] telmisartan at 37°C in 500 μl DMEM. Dissociation was then initiated by rapidly washing the cells three times with 500 μl fresh DMEM at 37°C. Cells were then incubated at 37°C for the indicated time periods up to 240 min (that is 'washout time') with 500 μl DMEM either with or without 1 μM candesartan. Nonspecific binding was determined in the presence of unlabelled candesartan and since the nonspecific binding in these studies displayed a timewise dissociation (data not shown), these values were subtracted from total binding to yield specific binding.

Saturation binding studies. Cells were incubated at 37°C in 500 μl DMEM for 40 min with either [^{3}H] olmesartan (0.25–10 nM) or for 20 min with [^{3}H] telmisartan (0.5–15 nM). Nonspecific binding was obtained, as above, in the presence of 0.5 μM candesartan per 1 nM [^{3}H] olmesartan or 0.2 μM candesartan per 1 nM [^{3}H] telmisartan. The protein content was determined using a bicinchoninic acid protein assay (Pierce, Rockford, IL, USA).

Competition binding studies. Cells were preincubated for 30 min at 37°C in 450 μl DMEM either with an unlabelled antagonist (olmesartan, telmisartan or losartan) or without these antagonists (control binding). Then, 50 μl DMEM containing either [^{3}H] olmesartan (1.5 nM final concentration) or [^{3}H] telmisartan (5 nM final concentration) was immediately added and the cells were further incubated for 40 min at 37°C. The amount of specific binding after various time intervals was determined.

Measurement of inositol phosphate accumulation in CHO-hAT$_1$ cells

CHO-hAT$_1$ cells were first grown for 20 h in supplemented DMEM with 1 μCi ml^{-1} myo-[^{3}H] inositol, then washed twice with ~500 μl DMEM. Cells remained in 400 μl DMEM containing 10 mM LiCl for 15 min at 37°C.

Olmesartan and telmisartan preincubation experiments. Preincubation studies were initiated by adding 50 μl DMEM-LiCl medium either with the indicated concentrations of unlabelled olmesartan or telmisartan or without these antagonists (controls for basal and maximal IP production) and allowed to continue at 37°C for 30 min. Subsequent incubations with agonists were also initiated by adding 50 μl DMEM-LiCl medium with or without (control) the indicated concentrations of Ang II. Incubations continued at 37°C for only an additional 5 min.

Olmesartan and telmisartan co-incubation experiments. Co-incubation studies involved the simultaneous addition of olmesartan or telmisartan and Ang II in 100 μl DMEM-LiCl medium. Incubation proceeded at 37°C for 5 min.

Functional recovery experiments. Preincubation studies were initiated by the addition of 50 μl DMEM containing olmesartan (2 nM) or telmisartan (10 nM) or lacking an ARB (controls). Incubation continued at 37°C for 30 min. For washout, cells were washed three times with ~500 μl DMEM at 37°C and incubated for various periods of time at 37°C in 500 μl DMEM either with or without losartan (10 μM final concentration). Cells were then incubated for 5 min at 37°C with 450 μl fresh DMEM-LiCl medium with or without losartan (10 μM). The total time taken by these latter two incubations is referred to as the 'washout time'. Finally, 50 μl DMEM-LiCl medium with Ang II (10 μM) was added and the incubation was performed for 5 min at 37°C.

Measurement of inositol phosphate (IP, representing inositol mono-, bis- and trisphosphates) accumulation was performed at the end of each assay as described previously (Vanderheyden *et al*., 1999). Briefly, the plates were placed on ice and IP formation was stopped by aspiration of the medium and by the addition of 750 μl formic acid (10 mM) at 4°C. After 30 min, this solution was applied to a column containing 1 ml Bio-Rad anion exchange resin (AG 1 × 8, formate form, 200–400 mesh, Bio-Rad Laboratories, Nazareth, Belgium). To remove free inositol, the resin was first washed twice with 3 ml of formic acid (0.1 M). The inositol mono-, bis- and trisphosphates were then eluted with 3 ml formic acid (0.1 M) containing ammonium formate (0.8 M) and radioactivity was measured in a liquid scintillation counter after the addition of 10 ml of scintillation liquid (Ultima-flo-AF, Packard, Groningen, The Netherlands).

Data analysis

Nonspecific radioligand binding determined using candesartan was subtracted from the total binding to yield specific binding for [^{3}H] olmesartan and [^{3}H] telmisartan. All parameters were determined by using nonlinear regression analysis of the experimental data with GraphPad Prism software (GraphPad Software Inc., San Diego, CA, USA). Kinetic data are the mean ± s.e.m. of three separate experiments with triplicate determinations each. Other data are the mean ± s.e.m. of three separate experiments with duplicate determinations each. Significant differences between two means were assessed by two-tailed *t*-tests with $P<0.05$ as the significance level.

Materials

Olmesartan [RNH-6270; 4-(1-hydroxy-1-methylethyl)-2-propyl-1-{4-[2-(tetrazol-5-yl)phenyl]phenyl}methylimidazol-5-carboxylic acid] was synthesized and radiolabelled (79 Ci mM^{-1}) by Daiichi-Sankyo Co., Ltd (Tokyo, Japan). Telmisartan [BIBR277; 4′-[[2-*n*-propyl-4-methyl-6-(1-methylbenz-imidazol-2-yl)benzimidazol-1-yl]methyl]biphenyl-2-carboxylic acid] was synthesized by Forest Laboratories Inc. (Parsippany, NJ, USA) and radiolabelled as [^{3}H] telmisartan (35 Ci mM^{-1}) by Perkin-Elmer (Shelton, CT, USA). Myo-[^{3}H] inositol (1.0 μCi ml^{-1}) was obtained from Amersham Biosciences (Buckinghamshire, UK), while candesartan [CV-11974; 2-ethoxy-1-[(2′-(1*H*-tetrazol-5-yl)biphenyl-4-yl)methyl]-1H-benzimidazoline-7-carboxylic acid] and losartan [DuP 753; 2-*n*-butyl-4-chloro-5-hydroxymethyl-1-[(2′-(1*H*-tetrazol-5-yl)-biphenyl-4-yl)methyl]imidazole] were obtained from AstraZeneca (Mölndal, Sweden) and Ang II from Neosystem (Strasbourg, France). All other chemicals were of the highest grade commercially available.

Results

Radioligand binding studies

[^{3}H] Olmesartan and [^{3}H] telmisartan binding. Specific binding of [^{3}H] olmesartan (1.5 nM) and [^{3}H] telmisartan (1.5 nM) to intact CHO-hAT$_1$ cells at 37°C increased with time until a plateau was reached, within 30 min for [^{3}H] olmesartan and 20 min for [^{3}H] telmisartan (Figures 1a and c, respectively). Fitting these association data to an exponential function resulted in pseudo-first-order association rate constants (k_{obs}; Table 1), yielding a $t_{1/2}$ value of 4.3 ± 0.7 min for olmesartan (1.5 nM) and, for telmisartan (1.5 nM), a $t_{1/2}$ value of 6.8 ± 1.3 min. The binding of [^{3}H] telmisartan at the higher concentration (5 nM; Figure 1c) provided a higher k_{obs} (Table 1) with a consequently shorter $t_{1/2}$ of 3.2 ± 0.3 min ($P<0.05$). In long-term incubations, the specific binding of [^{3}H] telmisartan and olmesartan (5 nM) remained stable for ~240 min (data not shown). The nonspecific binding of

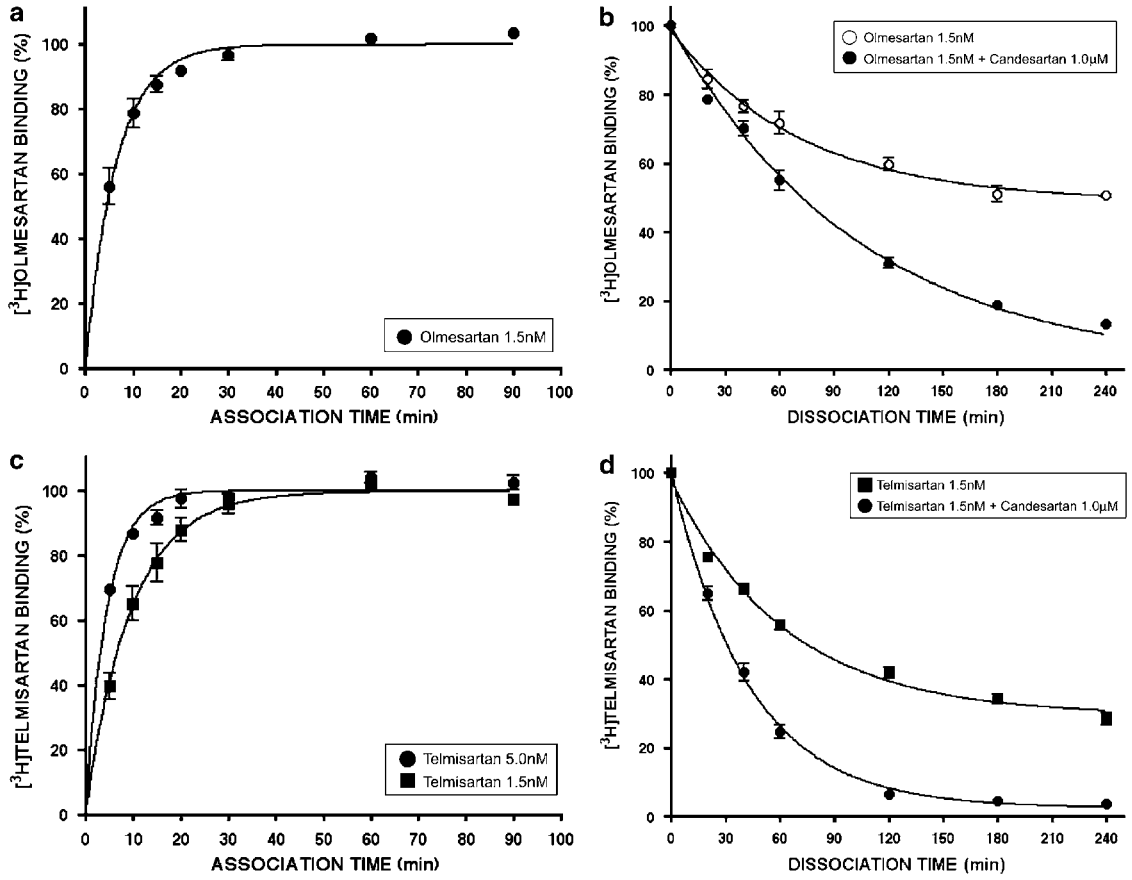

Figure 1 The association and dissociation binding kinetics of [^{3}H] olmesartan and [^{3}H] telmisartan. Panels (**a**) and (**c**) describe the association binding of [^{3}H] olmesartan (1.5 nM) and [^{3}H] telmisartan (1.5 and 5.0 nM), respectively, to CHO-hAT_1 cells at 37°C as a function of incubation time. Panel (**b**) describes the dissociation binding of [^{3}H] olmesartan (1.5 nM) from cells that were incubated for 30 min, washed and further incubated in fresh medium or in medium containing 1.0 μM candesartan. Panel (**d**) describes the dissociation binding of [^{3}H] telmisartan (1.5 nM) in fresh medium or medium containing 1.0 μM candesartan. Remaining binding was measured at the indicated time intervals up to 240 min. Data (mean $\pm$ s.e.m. from three experiments, three determinations each) refer to specific binding, and are given as the percentage of binding at equilibrium (**a** and **c**) or binding immediately after the wash step (**b** and **d**). Calculated parameters are given in Table 1.

Table 1 Kinetic parameters for [^{3}H] olmesartan and [^{3}H] telmisartan binding to CHO-hAT_1 cells

	Concentration [L] (nM)	k_{obs} *(M^{-1} min^{-1})*	k_{-1} *(min^{-1})*	K_D *(nM)*
[^{3}H] Olmesartan	1.5	0.168 $\pm$ 0.027	0.0096 $\pm$ 0.0002	0.091
[^{3}H] Telmisartan	1.5	0.105 $\pm$ 0.018	ND	0.12
[^{3}H] Telmisartan	5.0	0.218 $\pm$ 0.018*	0.0237 $\pm$ 0.0018	0.0021

k_{obs} and k_{-1} values were obtained from the [^{3}H] olmesartan and [^{3}H] telmisartan association and dissociation curves shown in Figures 1a–d.
Data are mean $\pm$ s.e.m. of three experiments, three determinations each. The equilibrium dissociation constant K_D was calculated as: [L]. $k_{-1}/(k_{obs}-k_{-1})$.
ND = no determination. *$P<0.0058$ (two-tailed *t*-test, 95% confidence interval) compared with value for 1.5 nM telmisartan.

[^{3}H] olmesartan was less than 5% of total binding, and no specific binding could be detected when the same experiment was performed using native CHO-K1 cells (that is, cells that do not express AT_1 receptors; data not shown). However, unlike [^{3}H] olmesartan, at concentrations of 1.5 and 5 nM, nonspecific binding of [^{3}H] telmisartan accounted for 15 and 25%, respectively, of the total binding.

In the dissociation experiments, dissociation at 37°C was monitored for different periods of time under two different experimental conditions. First, cells were incubated further with fresh medium containing candesartan (1.0 μM). At this concentration, AT_1 receptors are saturated and candesartan effectively prevents the potential rebinding of free [^{3}H] olmesartan or free [^{3}H] telmisartan to the AT_1 receptor. Such a phenomenon, which results from the high affinity these antagonists have for the AT_1 receptor, interferes with the measurement of ligand dissociation rates (Vanderheyden *et al*., 2000b). In the presence of 1.0 μM candesartan, the specific binding of both [^{3}H] olmesartan (Figure 1b) and [^{3}H] telmisartan (Figure 1d) decreased exponentially and a

greater majority of the sites were liberated at the end of the experiment, that is, after 240 min. The corresponding dissociation rate constants (k_{-1}) are given in Table 1 and yielded a $t_{1/2}$ of 65 ± 11 min for [^{3}H] olmesartan and, for [^{3}H] telmisartan, a $t_{1/2}$ of 29.4 ± 2 min.

In the second experimental procedure, dissociation of the radioligands from their specific binding sites on cells was examined by incubation in fresh medium alone. Under this condition, specific binding of both [^{3}H] olmesartan and [^{3}H] telmisartan followed a more complex pattern. When the resulting curves were fitted with an exponential function, a plateau of $48.6 \pm 3.2\%$ ($n = 3$) of the initial binding was produced by [^{3}H] olmesartan (Figure 1b). A plateau of $29.3 \pm 2.1\%$ ($n = 3$) was produced by [^{3}H] telmisartan (Figure 1d).

The specific binding of both [^{3}H] olmesartan and [^{3}H] telmisartan to intact CHO-hAT_1 cells is a saturable process. In agreement with a simple bimolecular ligand–receptor interaction, the amount of bound radioligand increased with its free concentration according to a hyperbolic function (Figures 2a and b, respectively). Such saturation binding curves reveal a single class of binding site for each radioligand and fitting the data to a hyperbolic function gave similar B_{max} (the maximum amount of drug which can bind specifically to the receptors) values (697 ± 22 fmol mg^{-1} protein for [^{3}H] olmesartan and 690 ± 18 fmol mg^{-1} protein for [^{3}H] telmisartan). These experiments yielded an equilibrium dissociation constant (K_D) for olmesartan of 0.18 ± 0.04 nM, which for a [^{3}H] olmesartan concentration ([L]) of 1.5 nM, was about twice the K_D value calculated from the kinetic parameters ($K_D = [L] \cdot k_{-1}/(k_{obs} - k_{-1})$; see Table 1) of 0.091 nM. For high-affinity radioligands, such a difference may be related to the long delay required for equilibrium binding to be attained at low radioligand concentrations. Hence, the K_D values obtained from saturation binding studies with high-affinity radioligands like [^{3}H] olmesartan are likely to underestimate their true affinity. The K_D for [^{3}H] telmisartan was 1.1 ± 0.4 nM, which is similarly double the K_D value of 0.61 nM, calculated from the kinetic parameters for a radioligand concentration ([L]) of 5 nM (see Table 1). In these saturation binding experiments, nonspecific [^{3}H] olmesartan binding was non-detectable; however, [^{3}H] telmisartan binding increased proportionally to its free concentration (data not shown).

The potency of olmesartan and telmisartan binding was compared with that of losartan in competitive binding experiments. As shown in Figures 3a and b, all tested unlabelled competitor ligands for the AT_1 receptor produced a concentration-dependent inhibition of the specific [^{3}H] olmesartan and [^{3}H] telmisartan binding. As expected for an homogenous class of binding sites and a simple bimolecular competitor–receptor interaction, the resulting competition binding curves were sigmoidal with Hill coefficients close to unity (1.0; data not shown). Based on the IC_{50} values from these studies (Table 2), unlabelled olmesartan was the most potent in displacing [^{3}H] olmesartan binding with unlabelled telmisartan about eight times less potent and losartan about 474 times less potent (Table 3).

Inhibition of [^{3}H] telmisartan binding was evaluated similarly. As shown in Figure 3b, maximal displacement of total [^{3}H] telmisartan binding by olmesartan, telmisartan and losartan occurred to the same extent. Hence, the nonspecific binding of telmisartan is a non-saturable process, at least for concentrations up to 10 μM. Competition binding curves were steep for all ligands and the IC_{50} values for olmesartan and telmisartan were markedly lower than that of losartan. The equilibrium dissociation constants for olmesartan ($K_i = 0.091$ nM; as calculated using the Cheng and Prusoff (1973) equation) and telmisartan ($K_i = 0.47$ nM) were similar to the K_D values for, respectively, [^{3}H] olmesartan and [^{3}H] telmisartan calculated from the kinetic and saturation binding experiments.

Ang II-induced IP production

Co-incubation experiments. Ang II produced a concentration-dependent increase of IP accumulation in CHO-hAT_1 cells, with an EC_{50} between 1.5 and 3.0 nM (taken from the control curves in Figures 4a and b) when given a 5 min incubation period at 37°C. In co-incubation experiments, under the same conditions, olmesartan (Figure 4a) produced a concentration-dependent rightward shift of the IP accumulation curve ($EC_{50} = 14.7 \pm 1.2$ and 175 ± 28 nM for 5 and 50 nM olmesartan, respectively). Telmisartan (Figure 4b) produced EC_{50} values of 13.7 ± 1.9 and 118 ± 19 nM at concentrations of 20 and 200 nM, respectively. Neither antagonist produced a depression of the maximal response (Figures 4a and b).

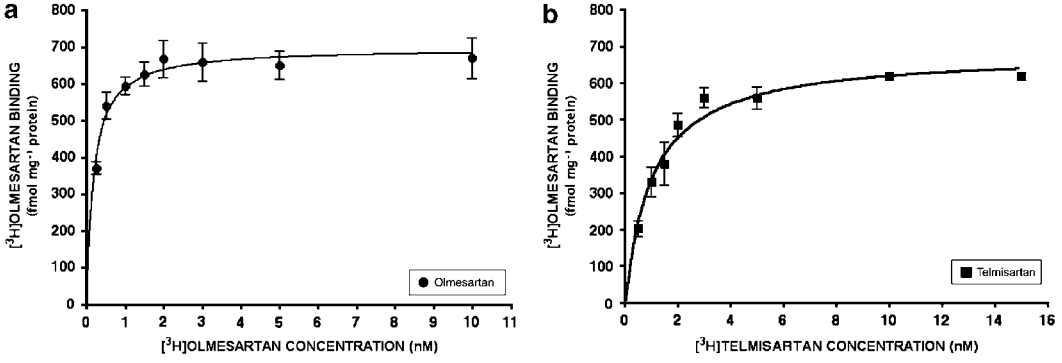

Figure 2 Saturation binding of [^{3}H] olmesartan and [^{3}H] telmisartan in CHO-hAT_1 cells. Cells were incubated for 40 and 20 min with increasing concentrations of [^{3}H] olmesartan (**a**) and [^{3}H] telmisartan (**b**), respectively, at 37°C. All data (mean ± s.e.m. from three experiments, two determinations each) refer to specific binding and are expressed as fmol mg^{-1} protein.

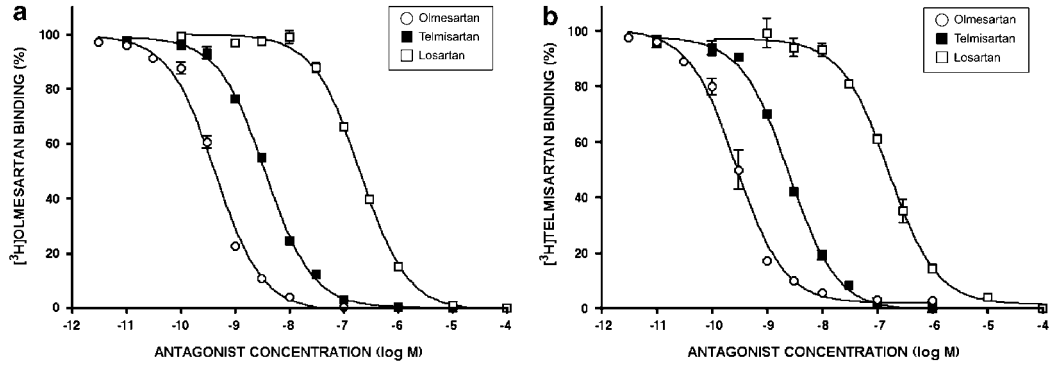

Figure 3 Competition binding experiments with [^{3}H] olmesartan (**a**) and [^{3}H] telmisartan (**b**). CHO-hAT_1 cells preincubated for 30 min at 37°C without (control binding) or with increasing concentrations of olmesartan, telmisartan or losartan were further incubated for 40 min with 1.5 nM [^{3}H] olmesartan (**a**). CHO-hAT_1 cells preincubated under identical conditions without (control binding) or with increasing concentrations of olmesartan, telmisartan or losartan were further incubated for 40 min with 5.0 nM [^{3}H] telmisartan (**b**). Data (mean ± s.e.m. from three experiments, two determinations each) refer to specific binding and are expressed as percent of control binding. Calculated IC_{50} values are given in Table 2.

Table 2 Competition binding IC_{50} values for unlabelled antagonists

Ligand	*[^{3}H] telmisartan*		*[^{3}H] olmesartan*	
	IC_{50} (nM)	*Potency ratio*	*IC_{50} (nM)*	*Potency ratio*
Olmesartan	0.28 ± 0.05	1.0	0.43 ± 0.02	1.0
Telmisartan	2.6 ± 0.1	9.3	3.6 ± 0.1	0.12
Losartan	160 ± 21	571	204 ± 11	0.0021

Values were calculated from the [^{3}H] olmesartan and [^{3}H] telmisartan competition binding curves shown in Figures 3a and b, respectively.
Data shown in the Table are means ± s.e.m. of three experiments, two determinations each.

Table 3 ARB AT_1 receptor interactions on CHO-hAT_1 cells

Ligand	*Receptor interaction* $I + R \leftrightarrow IR \leftrightarrow IR^*$		*Dissociation* $t_{1/2}$ *(min)*	*Binding potency*
	Fast-dissociating complexes (%)	*Slow-dissociating complexes (%)*		
Olmesartan	15	85	76	1
Telmisartan	30	70	25	0.12
EXP3174	30	70	30	0.45

Abbreviations: I = initial ARB; R = receptor. The initial interaction yields a loose, fast-dissociating/surmountable complex (IR), which may subsequently be transformed to a slow-dissociating, tight binding/insurmountable complex (IR*).
The percentages of fast- and slow-dissociating complexes refer to surmountable and insurmountable effects of the ARBs on Ang II-mediated responses. Dissociation half-lives are calculated from radioligand binding and/or functional experiments. Their potencies are from competition binding experiments (data for EXP3174 are from Vauquelin *et al.*, 2006).

Preincubation experiments. In contrast, preincubation of the cells for 30 min with either olmesartan (0.5 or 100 nM) or telmisartan (3 or 100 nM) decreased the maximal response to subsequently added Ang II by 41 ± 7 and 80 ± 2%, respectively, for olmesartan (Figure 5a) and by 52 ± 7 and 66 ± 3%, respectively, for telmisartan (Figure 5b). At the lowest olmesartan concentration tested, there was a minimal effect on the EC_{50} of Ang II ($EC_{50} = 2.2 \pm 0.3$ nM; that is ~1.4-fold shift) but at a concentration of 100 nM, a marked rightward shift of the Ang II concentration–response curve was observed ($EC_{50} = 387 \pm 48$ nM; that is, a 257-fold shift). Similarly, telmisartan at the lowest concentration tested did not affect the EC_{50} of Ang II ($EC_{50} = 3.7 \pm 0.3$ nM; that is, ~2.4-fold shift) but at 100 nM, it produced a marked rightward shift of the Ang II concentration–response curve ($EC_{50} = 151 \pm 33$ nM; that is, ~100-fold shift).

To better quantify the maximal insurmountable effect of olmesartan and telmisartan, cells were preincubated with increasing concentrations of either antagonist (0.01–30 μM for olmesartan and 0.01–10 μM for telmisartan) and then further incubated for 5 min with an elevated concentration of Ang II (10 μM). The resulting olmesartan and telmisartan concentration–inhibition curves were biphasic (Figure 6) characterized by an initial steep reduction in the response, followed by a plateau response phase and then a further reduction of the response until complete abolition resulted at high concentrations. It should be noted that due to the absence of 'receptor reserve' in the stably transfected AT_1 receptor-expressing CHO cells (Lew *et al.*, 2001; Vauquelin *et al.*, 2001a, b; Le *et al.*, 2005), the plateau component of the curves shown in Figure 6 provides a convenient way to determine the maximal degree of insurmountable inhibition by AT_1 receptor antagonists (Fierens *et al.*, 1999b). In the present experiment, 89.4 ± 0.7% of the olmesartan-AT_1 receptor complexes were found to be insurmountable, while only 69.0 ± 1.0% of the telmisartan-AT_1 receptor complexes were insurmountable.

AT_1 receptor functional recovery studies. Further investigation into the dissociation properties of olmesartan and telmisartan from the AT_1 receptor was conducted using indirect kinetic methods, by monitoring the time-dependent restoration of Ang II responses in functional 'washout' experiments. To this end, cells were first incubated for 30 min at 37°C with olmesartan (2 nM) or for 20 min at 37°C with telmisartan (5 nM), rapidly washed to remove free antagonist, and further exposed to fresh medium or medium containing losartan (10 μM) for the indicated periods of time before measuring IP production resulting from Ang II (10 μM) application. In

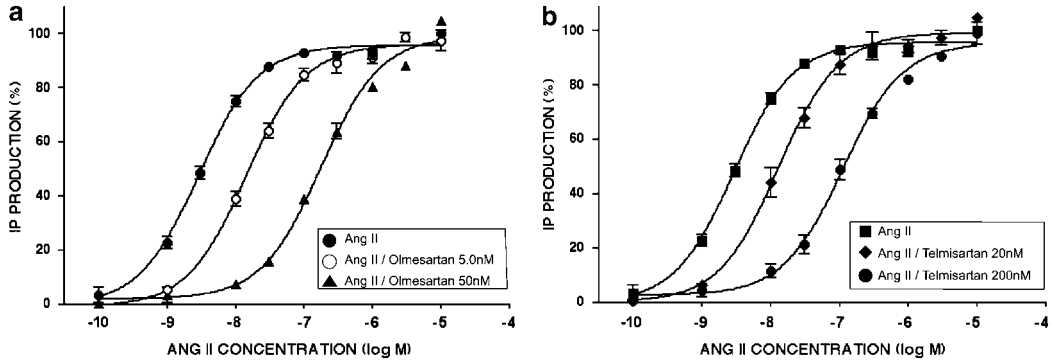

Figure 4 The effect of either olmesartan or telmisartan co-incubation on Ang II-mediated intracellular inositol phosphate accumulation in CHO-hAT_1 cells. Cells were incubated for 5 min at 37°C with increasing concentrations of Ang II, either alone or in the presence of 5 or 50 nM olmesartan (**a**); or alone or in the presence of 20 or 200 nM telmisartan (**b**). Data (mean ± s.e.m. from three experiments, two determinations each) refer to Ang II-mediated IP accumulation above basal levels and are expressed as percent of maximal accumulation in the absence of either olmesartan or telmisartan.

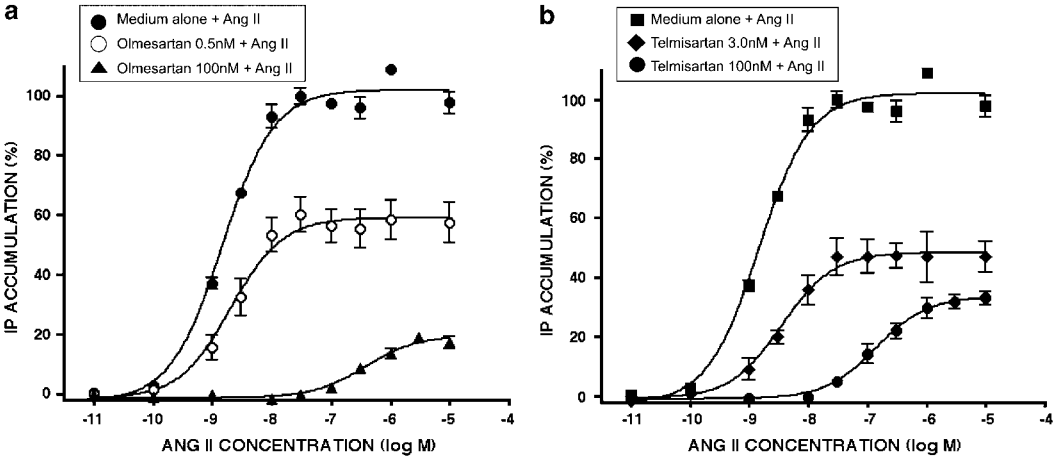

Figure 5 The effect of preincubation of either olmesartan or telmisartan on Ang II-mediated inositol phosphate accumulation in CHO-hAT_1 cells. In panel (**a**), cells were preincubated with medium alone or with 0.5 or 100 nM olmesartan for 30 min at 37°C and then further incubated for 5 min with increasing concentrations of Ang II. In panel (**b**), cells were preincubated with medium alone or with 3.0 or 100 nM telmisartan for 30 min at 37°C and then further incubated for 5 min with increasing concentrations of Ang II. Data are expressed as percent of maximal IP accumulation in control cells.

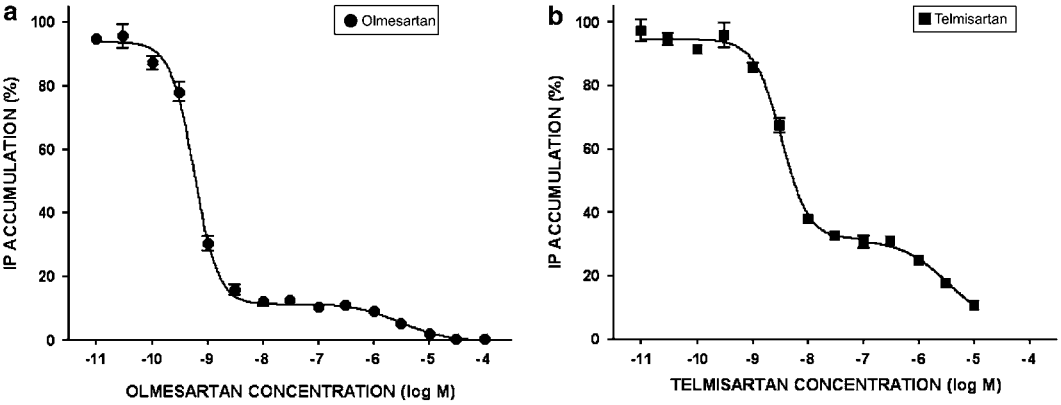

Figure 6 Concentration–inhibition curves for olmesartan (**a**) and telmisartan (**b**) on Ang II-mediated inositol phosphate (IP) accumulation. CHO-hAT_1 cells were preincubated for 30 min at 37°C without (control) or with increasing concentrations of either olmesartan or telmisartan and then further incubated for 5 min with 10 μM Ang II. Data (mean ± s.e.m. from three experiments, two determinations each) refer to Ang II-mediated IP accumulation over basal levels, and are expressed as percent of maximal IP accumulation in the absence of either olmesartan or telmisartan. Calculated parameters are discussed in the Results section and given in Table 3.

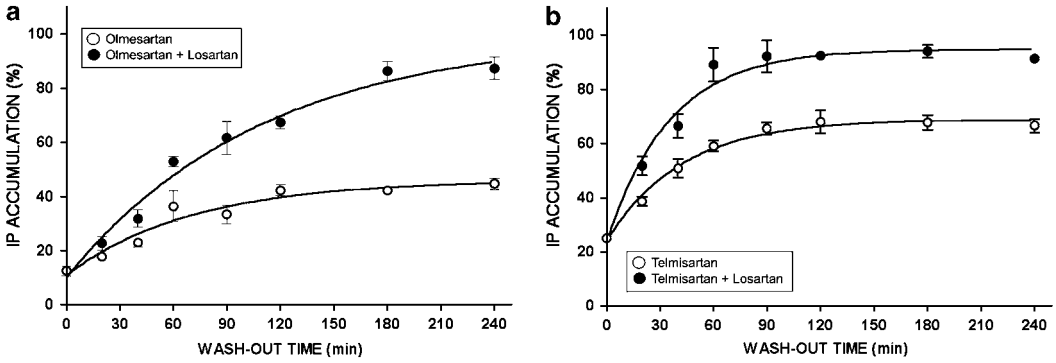

Figure 7 Time-dependent reversal of the insurmountable inhibition by olmesartan (**a**) and telmisartan (**b**) of Ang II-mediated inositol phosphate (IP) accumulation. CHO-hAT_1 cells were preincubated for 30 min without (control) or with olmesartan (2 nM) or telmisartan (10 nM), washed, and further incubated with fresh medium or medium containing losartan (10 μM) for the indicated time periods before final incubation with 10 μM Ang II for 5 min. IP accumulation was measured in the absence or presence of losartan in the washout medium. Data (mean $\pm$ s.e.m. from three experiments, three determinations each) refer to Ang II-mediated IP accumulation over basal levels and are expressed as percent of accumulation at the corresponding time points in the absence of either olmesartan or telmisartan.

close agreement with the partial insurmountable effect of olmesartan and telmisartan in the preceding experiments (Figures 5a and b), Ang II produced either a 13 ± 2 or $25 \pm 2\%$ accumulation, respectively, of IP under control conditions (that is, after preincubation without either olmesartan or telmisartan) at the onset of washout (Figures 7a and b).

The presence of losartan (10 μM) in the washout medium is sufficient to prevent the potential rebinding of either olmesartan or telmisartan to the receptor but does not depress stimulation of the AT_1 receptor by a high concentration of Ang II (Vanderheyden *et al*., 1999, 2000a).

Under these conditions, the Ang II response increased exponentially with the washout time lasting until full recovery was achieved for olmesartan (that is $100 \pm 4\%$ of the control response; Figure 7a) and telmisartan (that is $95 \pm 2\%$ of the control IP accumulation). The recovery rate constant (k_{recov}) determined for olmesartan was $0.0091 \pm 0.0010\,M^{-1}\,min^{-1}$, which yields a $t_{1/2}$ of 75.9 min. This value is in good agreement with the dissociation rate constant determined for [^{3}H] olmesartan in the corresponding radioligand binding studies (see above). Similarly, the recovery rate constant (k_{recov}) for telmisartan was $0.0283 \pm 0.0023\,M^{-1}\,min^{-1}$, yielding a $t_{1/2}$ of 24.5 min. When the washout proceeded in the absence of losartan, the Ang II response similarly increased in a time-dependent manner; however, AT_1 receptor recovery was not complete. The IP accumulation response compared with that of controls was only $46 \pm 2\%$ for olmesartan and $69 \pm 1\%$ for telmisartan (Figures 7a and b, respectively).

These studies confirm that losartan effectively prevents the rebinding of olmesartan and telmisartan to the AT_1 receptor, and that the recovery half-lives correspond to the dissociation half-lives of these insurmountable antagonists determined directly by the radioligand binding studies.

Discussion

The present study is the first to describe the kinetic and functional binding properties of the non-peptide ARB olmesartan in CHO cells expressing human AT_1 receptors, and compare these properties to another ARB, telmisartan. It was shown that olmesartan is a competitive antagonist, displaying high affinity, slow dissociation and a high degree of insurmountability for these receptors. Interestingly, nonspecific binding of [^{3}H] olmesartan to the CHO-hAT_1 cells was virtually absent and specific binding likely only occurs to the AT_1 receptors, as it could be fully displaced by other unlabelled ARBs (Figure 3a). While the specific binding of [^{3}H] telmisartan to intact cells also occurred at AT_1 receptors, with complete displacement by other unlabelled ARBs (Figure 3b), there was a greater degree of nonspecific binding of this ARB. In a manner similar to that observed in previous competition binding experiments with [3 H] candesartan, [^{3}H] valsartan, [^{3}H] irbesartan and [^{3}H] angiotensin (Fierens *et al*., 1999a; Vanderheyden *et al*., 1999, 2000c; Verheijen *et al*., 2000), olmesartan and telmisartan binding was more potent than that of losartan in this study (Figures 3a and b; Table 2). However, comparative clinical data are not available for olmesartan versus telmisartan. Therefore, with current evidence, it is unclear whether these differences in binding properties translate into variations in clinical characteristics among the ARBs.

In a manner similar to previously tested ARBs (Fierens *et al*., 1999a; Vanderheyden *et al*., 2000c; Verheijen *et al*., 2000), olmesartan and telmisartan both produced concentration-dependent rightward shifts of the Ang II concentration–response curve in co-incubation experiments, characteristic of a competitive receptor antagonist. Interestingly, however, when cells were preincubated with either olmesartan or telmisartan, the drugs behaved as 'partial' insurmountable antagonists. The inhibition patterns observed for olmesartan and telmisartan (see Figure 5) were similar to those observed earlier for other ARBs (Fierens *et al*., 1999a; Verheijen *et al*., 2000) and reveal that, as their concentration rises, they produce an initial decline of the maximal response until a specific limit is reached, followed by a rightward shift of the Ang II concentration–response curve. The maximal degree of insurmountability of olmesartan was very similar in the different preincubation-based

experiments (~80% in Figure 5a, ~89% in Figure 6a and ~87% in Figure 7a). A comparable degree of insurmountable antagonism with olmesartan was also observed in studies of Ang II-mediated contraction of isolated guinea-pig aortas (Mizuno *et al*., 1995). The maximal degree of insurmountability of telmisartan was also very similar and consistently lower than for olmesartan in the different experiments (~66% in Figure 5b, ~69% in Figure 6b and ~75% in Figure 7b).

A two-step, two-state model (Vauquelin *et al*., 2001b, c, d), whereby the initial ARB (I) receptor (R) interaction yields a fast reversible/surmountable complex (IR) and where this complex may subsequently adopt a tight binding/insurmountable state (IR*), has already been proposed to explain the competitive and partially insurmountable properties of previously tested ARBs (that is irbesartan, valsartan, EXP3174 and candesartan), and readily explains the behaviour of olmesartan and telmisartan in functional experiments in this study.

$$I + R \underset{k_{-1i}}{\overset{k_{1i}}{\rightleftharpoons}} I.R \underset{k_{-2i}}{\overset{k_{2i}}{\rightleftharpoons}} I.R^*$$

To explain the partial insurmountability observed with these ARBs, this model stipulates that the IR↔IR* interconversion must be a reversible process and must reach an equilibrium. As such, only some of the antagonist-AT_1 receptor complexes reside in the IR* state, while the remaining complexes are in the IR state (Fierens *et al*., 1999b; Vauquelin *et al*., 2001b, d). The surmountable behaviour of losartan can most likely be attributed to its inability to sufficiently stabilize the IR* state. From a structural point of view, olmesartan (Figure 8) and many of the previously tested ARBs (Berellini *et al*., 2005) possess an acidic tetrazole group at the 2′-position of their biphenylmethyl moiety (Mire *et al*., 2005). Based on simulation studies, it was proposed that this moiety plays an essential role in the initial drug–receptor binding process (Vauquelin *et al*., 2001c). Because the initial I + R↔IR interaction is similar for these ARBs, differences in kinetic binding properties likely result from the ability of the ARB to stabilize the IR* complex.

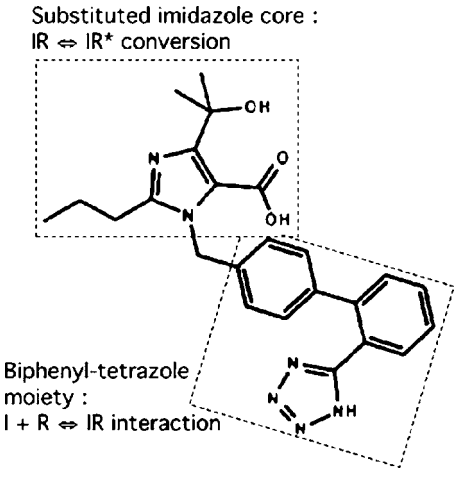

Figure 8 The chemical structure of olmesartan showing the biphenyltetrazole moiety and the substituted imidazole core. These structural substituents may contribute to its AT_1 receptor binding profile (Mire *et al*., 2005).

The model also predicts that the degree of insurmountability, the drug–receptor dissociation $t_{1/2}$ and the overall affinity for the AT_1 receptor are positively correlated to one another (Vauquelin *et al*., 2001c, d). This positive correlation was observed for previously tested ARBs (Vauquelin *et al*., 2006) and in the present study only for olmesartan.

Competition binding studies on CHO-hAT_1 cells with various radioligands revealed the same order of potencies for biphenyl tetrazole-based ARBs (that is candesartan > EXP3174 > valsartan > irbesartan ≫ losartan), and it has consistently been found that EXP3174 is only about two times less potent than candesartan (Fierens *et al*., 1999a; Vanderheyden *et al*., 1999, 2000c; Verheijen *et al*., 2000). Despite having the same dissociation rate and extent of insurmountability as EXP3174, telmisartan was less potent based on the present study (Table 3). This is likely to reflect a lower potency at the level of the initial I + R↔IR interaction, as supported by the finding that the k_{-1i}/k_{1i} ratio (Vauquelin *et al*., 2001b) was ~4.5-times higher for telmisartan than for EXP3174, that is, ~10 versus ~2.2 nM, respectively (unpublished observation). In comparison, calculated k_{-1i}/k_{1i} ratios were found to be very similar for EXP3174 and other biphenyl-tetrazole-based ARBs (Vauquelin *et al*., 2001b), consistent with the proposal that the biphenyl moiety of these molecules plays an essential role in the initial binding process (Vauquelin *et al*., 2001c). The present findings with telmisartan are still compatible with such a model if one assumes that the replacement of the tetrazole substituent of the biphenyl moiety by a carboxyl group decreases the potency of this initial interaction.

The insurmountable behaviour of olmesartan in the present study appears better than telmisartan. From a structural point of view, the insurmountability of ARBs like candesartan and EXP3471 can be clearly linked to the presence of a carboxyl group at their imidazole core. Indeed, this group is either absent or esterified in their prodrugs, candesartan cilexetil and losartan, and these agents are unable to display insurmountable antagonism (Noda *et al*., 1993; Mizuno *et al*., 1995). Yet, telmisartan, valsartan and other ARBs (Criscione *et al*., 1993; Wienen *et al*., 1993; Schambye *et al*., 1994; De Arriba *et al*., 1996) also show insurmountable behaviour despite the absence of a carboxylic group. This suggests that besides acidic function moieties, ARBs also utilize other pharmacophores at their imidazole core to stabilize the IR* state of interaction. So, while the carboxyl group at the imidazole core of olmesartan (Figure 8) could contribute to its insurmountable behaviour, other substituents (for example the hydroxyisopropyl group and the isopropyl group) could further stabilize the IR* complex and/or be necessary for a correct spatial orientation of the carboxyl group (Mire *et al*., 2005).

The sigmoidal competition binding curves (see Figure 3) and the monoexponential dissociation curves (Figures 1 and 2) suggest that [^{3}H] olmesartan and [^{3}H] telmisartan-labelled AT_1 receptors behave uniformly, which is in apparent contrast to the two-step, two-state model. However, the dissociation of [^{3}H] olmesartan (Figure 1b) and of [^{3}H]

telmisartan (Figure 1d) occur at the same rate as the disappearance of their insurmountable effects in the functional 'washout' experiments, that is, with a $t_{1/2}$ of ~72 and ~76 min, respectively, for olmesartan (Figure 7a) and ~30 and ~25 min, respectively, for telmisartan (Figure 7b). Since these binding studies were performed under the same conditions as the functional assays, results from both can be objectively compared. The similarity suggests that the observed [^{3}H] olmesartan and [^{3}H] telmisartan binding only encompasses the insurmountable IR* complexes and that the surmountable IR* complexes are too short-lived to be detected by radioligand binding.

Previously, the dissociation rate of [^{3}H] telmisartan has been estimated in rat vascular smooth muscle cells under similar conditions to those used in the present study, with a $t_{1/2}$ of ~70–75 min, or about ~2.5 times slower than in our studies(Maillard *et al.*, 2002). Similar steps were taken to minimize experimental and other factors that are recognized to affect ARB dissociation rates. Consequently, the reason for the different dissociation rates is not entirely clear, but one hypothesis may be that the binding properties of [^{3}H] telmisartan differ slightly between rat and human AT_1 receptors. More recently, even slower telmisartan dissociation (that is, $t_{1/2} = 213$ min) was reported by Kakuta *et al.* (2005). However, the methods used differed, so these data cannot be compared with data from the present study.

Olmesartan displayed appreciable rebinding to CHO-hAT_1 cells, both in the [^{3}H] olmesartan dissociation and functional recovery experiments. The *in vivo* implications of antagonist rebinding phenomena have yet not been explored in detail but, together with the slow dissociation of olmesartan from the AT_1 receptor, its rebinding could potentially contribute to the marked long-lasting antihypertensive efficacy observed in the clinic (Smith *et al.*, 2005). Despite its 10-fold lower affinity, telmisartan also displayed some rebinding-like behaviour in the present experiments. Given that telmisartan is highly hydrophobic and displays a significant amount of nonspecific binding (~25% of total binding; data not shown), it is not clear whether this behaviour represents rebinding of telmisartan molecules in solution or a more complicated process involving a membrane lipid-associated pool of molecules (Panek *et al.*, 1995; Zoumpoulakis *et al.*, 2003).

In conclusion, in the present study with AT_1 receptor-expressing CHO cells, olmesartan and telmisartan were found to be competitive and partially insurmountable antagonists. As with the earlier tested biphenyl-tetrazole ARBs, the olmesartan-AT_1 and telmisartan-AT_1 receptor interactions can be described by a two-state process with the initial formation of a loose complex (IR) and its subsequent transformation into a tight binding complex (IR*). Telmisartan compares well with EXP3174 (the active metabolite of losartan) with regard to the degree of insurmountability and dissociation rate. Yet, telmisartan displays lower affinity, presumably because its biphenyl moiety contains a carboxyl substituent instead of a tetrazole group. On the other hand, the high degree of insurmountability, slow dissociation and high affinity of olmesartan for its receptor can be attributed to its ability to stabilize IR* via the carboxyl group, and possibly other substituents, of its imidazole core.

Acknowledgements

These studies were sponsored by Forest Laboratories Inc., New Jersey and Daiichi-Sankyo Inc., Parsippany, New Jersey, USA. Additional support was provided by the Fonds voor Wetenschappelijk Onderzoek Vlaanderen.

Conflict of interest

Georges Vauquelin has received a research grant from Daiichi Sankyo Inc. Michael Pugsley is a former employee of Forest Laboratories. Minh Tam Le and Isabelle Van Liefde have none to disclose.

References

Berellini G, Cruciani G, Mannhold R (2005). Pharmacophore, drug metabolism, and pharmacokinetics models on non-peptide AT1, AT2, and AT1/AT2 angiotensin II receptor antagonists. *J Med Chem* **48**: 4389–4399.

Cazaubon C, Gougat J, Bousquet F, Guiraudou P, Gayraud R, Lacour C *et al.* (1993). Pharmacological characterization of SR 47436, a new nonpeptide AT1 subtype angiotensin II receptor antagonist. *J Pharmacol Exp Ther* **265**: 826–834.

Cheng Y, Prusoff WH (1973). Relationship between the inhibition constant (K1) and the concentration of inhibitor which causes 50 per cent inhibition (I50) of an enzymatic reaction. *Biochem Pharmacol* **22**: 3099–3108.

Criscione L, de Gasparo M, Buhlmayer P, Whitebread S, Ramjoue HP, Wood J (1993). Pharmacological profile of valsartan: a potent, orally active, nonpeptide antagonist of the angiotensin II AT1-receptor subtype. *Br J Pharmacol* **110**: 761–771.

De Arriba AF, Gomez-Casajus LA, Cavalcanti F, Almansa C, Garcia-Rafanell J, Forn J (1996). *In vitro* pharmacological characterization of a new selective angiotensin AT1 receptor antagonist, UR-7280. *Eur J Pharmacol* **318**: 341–347.

de Gasparo M, Catt KJ, Inagami T, Wright JW, Unger T (2000). International union of pharmacology. XXIII. The angiotensin II receptors. *Pharmacol Rev* **52**: 415–472.

Fierens F, Vanderheyden PM, De Backer JP, Vauquelin G (1999a). Binding of the antagonist [^{3}H]candesartan to angiotensin II AT1 receptor-transfected (correction of tranfected) Chinese hamster ovary cells. *Eur J Pharmacol* **367**: 413–422.

Fierens FL, Vanderheyden PM, De Backer JP, Vauquelin G (1999b). Insurmountable angiotensin AT1 receptor antagonists: the role of tight antagonist binding. *Eur J Pharmacol* **372**: 199–206.

Gavras H (1999). Historical evolution of angiotensin II receptor blockers: therapeutic advantages. *J Am Soc Nephrol* **10** (Suppl 12): S255–S257.

Kakuta H, Sudoh K, Sasamata M, Yamagashi S (2005). Telmisartan has the strongest binding affinity to angiotensin II type 1 receptor: comparison with other angiotensin II type 1 receptor blockers. *Int J Clin Pharmacol* **25**: 41–46.

Koike H, Konse T, Sada T, Ikeda T, Hyogo A, Hinman D *et al.* (2003). Olmesartan medoximil, a novel potent angiotensin II blocker. *Annual Report Sankyo Research Laboratories* **55**: 1–91.

Laeis P, Puchler K, Kirch W (2001). The pharmacokinetic and metabolic profile of olmesartan medoxomil limits the risk of clinically relevant drug interaction. *J Hypertens Suppl* **19**: S21–S32.

Le MT, De Backer JP, Hunyady L, Vanderheyden PM, Vauquelin G (2005). Ligand binding and functional properties of human angiotensin AT1 receptors in transiently and stably expressed CHO-K1 cells. *Eur J Pharmacol* **513**: 35–45.

Lew M, Christopoulos A, Ziogas J (2001). Insurmountable AT1 receptor antagonism: message in a model? *Trends Pharmacol Sci* **22**: 555–557.

Maillard MP, Perregaux C, Centeno C, Stangier J, Wienen W, Brunner HR *et al.* (2002). *In vitro* and *in vivo* characterization of the activity

of telmisartan: an insurmountable angiotensin II receptor antagonist. *J Pharmacol Exp Ther* **302**: 1089–1095.

Manohar P, Pina IL (2003). Therapeutic role of angiotensin II receptor blockers in the treatment of heart failure. *Mayo Clin Proc* **78**: 334–338.

Mire DE, Silfani TN, Pugsley MK (2005). A review of the structural and functional features of olmesartan medoxomil, an angiotensin receptor blocker. *J Cardiovasc Pharmacol* **46**: 585–593.

Mizuno M, Sada T, Ikeda M, Fukuda N, Miyamoto M, Yanagisawa H *et al.* (1995). Pharmacology of CS-866, a novel nonpeptide angiotensin II receptor antagonist. *Eur J Pharmacol* **285**: 181–188.

Mochizuki S, Sato T, Furuta K, Hase K, Ohkura Y, Fukai C *et al.* (1995). Pharmacological properties of KT3-671, a novel nonpeptide angiotensin II receptor antagonist. *J Cardiovasc Pharmacol* **25**: 22–29.

Neubig RR, Spedding M, Kenakin T, Christopoulos A (2003). International union of pharmacology committee on receptor nomenclature and drug classification. XXXVIII. Update on terms and symbols in quantitative pharmacology. *Pharmacol Rev* **55**: 597–606.

Noda M, Shibouta Y, Inada Y, Ojima M, Wada T, Sanada T *et al.* (1993). Inhibition of rabbit aortic angiotensin II (AII) receptor by CV-11974, a new nonpeptide AII antagonist. *Biochem Pharmacol* **46**: 311–318.

Norris K, Vaughn C (2003). The role of renin–angiotensin–aldosterone system inhibition in chronic kidney disease. *Expert Rev Cardiovasc Ther* **1**: 51–63.

Oparil S (2000). Newly emerging pharmacologic differences in angiotensin II receptor blockers. *Am J Hypertens* **13**: 18S–24S.

Panek RL, Lu GH, Overhiser RW, Major TC, Hodges JC, Taylor DG (1995). Functional studies but not receptor binding can distinguish surmountable from insurmountable AT1 antagonism. *J Pharmacol Exp Ther* **273**: 753–761.

Ries UJ, Mihm G, Narr B, Hasselbach KM, Wittneben H, Entzeroth M *et al.* (1993). 6-Substituted benzimidazoles as new nonpeptide angiotensin II receptor antagonists: synthesis, biological activity, and structure-activity relationships. *J Med Chem* **36**: 4040–4051.

Schambye HT, von Wijk B, Hjorth SA, Wienen W, Entzeroth M, Bergsma DJ *et al.* (1994). Mutations in transmembrane segment VII of the AT1 receptor differentiate between closely related insurmountable and competitive angiotensin antagonists. *Br J Pharmacol* **113**: 331–333.

Smith DH, Dubiel R, Jones M (2005). Use of 24-h ambulatory blood pressure monitoring to assess antihypertensive efficacy: a comparison of olmesartan medoxomil, losartan potassium, valsartan, and irbesartan. *Am J Cardiovasc Drugs* **5**: 41–50.

Timmermans PB (1999). Pharmacological properties of angiotensin II receptor antagonists. *Can J Cardiol* **15** (Suppl F): 26F–28F.

Vanderheyden PM, Fierens FL, De Backer J, Vauquelin G (2000a). Reversible and syntopic interaction between angiotensin receptor antagonists on Chinese hamster ovary cells expressing human angiotensin II type 1 receptors. *Biochem Pharmacol* **59**: 927–935.

Vanderheyden PM, Fierens FL, De Backer JP, Fraeyman N, Vauquelin G (1999). Distinction between surmountable and insurmountable selective AT1 receptor antagonists by use of CHO-K1 cells expressing human angiotensin II AT1 receptors. *Br J Pharmacol* **126**: 1057–1065.

Vanderheyden PM, Fierens FL, Vauquelin G (2000b). Angiotensin II type 1 receptor antagonists. Why do some of them produce insurmountable inhibition? *Biochem Pharmacol* **60**: 1557–1563.

Vanderheyden PM, Verheijen I, Fierens FL, Backer JP, Vauquelin G (2000c). Binding characteristics of [(3)H]-irbesartan to human recombinant angiotensin type 1 receptors. *J Renin Angiotensin Aldosterone Syst* **1**: 159–165.

Vauquelin G, Fierens F, Van Liefde I (2006). Interaction between the partially insurmountable antagonist valsartan and human recombinant angiotensin II type 1 receptors. *J Hypertens Suppl* **24**: S23–S30.

Vauquelin G, Fierens F, Verheijen I, Vanderheyden P (2001a). Insurmountable AT1 receptor antagonism: fitting models with experimental data. *Trends Pharmacol Sci* **22**: 557.

Vauquelin G, Fierens F, Verheijen I, Vanderheyden P (2001b). Insurmountable AT(1) receptor antagonism: the need for different antagonist binding states of the receptor. *Trends Pharmacol Sci* **22**: 343–344.

Vauquelin G, Fierens FLP, Verheijen I, Vanderheyden PML (2001c). Distinctions between non-peptide angiotensin II AT1 receptor antagonists. *J Renin Angiotensin Aldosterone Syst* **2**: S24–S31.

Vauquelin G, Morsing P, Fierens FL, De Backer JP, Vanderheyden PM (2001d). A two-state receptor model for the interaction between angiotensin II type 1 receptors and non-peptide antagonists. *Biochem Pharmacol* **61**: 277–284.

Vauquelin G, Van Liefde I, Vanderheyden P (2002). Models and methods for studying insurmountable antagonism. *Trends Pharmacol Sci* **23**: 514–518.

Verheijen I, Fierens FL, Debacker JP, Vauquelin G, Vanderheyden PM (2000). Interaction between the partially insurmountable antagonist valsartan and human recombinant angiotensin II type 1 receptors. *Fundam Clin Pharmacol* **14**: 577–585.

White WB, Lacourciere Y, Davidai G (2004). Effects of the angiotensin II receptor blockers telmisartan versus valsartan on the circadian variation of blood pressure: impact on the early morning period. *Am J Hypertens* **17**: 347–353.

Wienen W, Hauel N, Van Meel JC, Narr B, Ries U, Entzeroth M (1993). Pharmacological characterization of the novel nonpeptide angiotensin II receptor antagonist, BIBR 277. *Br J Pharmacol* **110**: 245–252.

Yanagisawa H, Amemiya Y, Kanazaki T, Shimoji Y, Fujimoto K, Kitahara Y *et al.* (1996). Nonpeptide angiotensin II receptor antagonists: synthesis, biological activities, and structure-activity relationships of imidazole-5-carboxylic acids bearing alkyl, alkenyl, and hydroxyalkyl substituents at the 4-position and their related compounds. *J Med Chem* **39**: 323–338.

Zoumpoulakis P, Daliani I, Zervou M, Kyrikou I, Siapi E, Lamprinidis G *et al.* (2003). Losartan's molecular basis of interaction with membranes and AT1 receptor. *Chem Phys Lipids* **125**: 13–25.